

Pt–Ce-soot generated from fuel-borne catalysts: soot oxidation mechanism

K. Krishna and M. Makkee*

Reactor and Catalysis Engineering, DelftChemTech, Delft University of Technology, Julianalaan 136, 2628 BL Delft, The Netherlands

Soot containing Ce-, Pt-, Pt–Ce-, Fe-, and Cu-fuel-borne catalysts is generated in a diesel engine, is characterised by XRD, and studied in oxidation with O_2 and $NO + O_2$ under various reaction conditions. Fe-, Pt–Ce- and Ce-soot are oxidised at lower temperature with O_2 , compared with Pt-soot, and the opposite trend is observed with $NO + O_2$. NO is oxidised to NO_2 more efficiently over Pt-soot and decreased the soot oxidation temperature by about 150 °C, compared with Ce-, Fe- or Pt–Ce-soot. On the other hand, NO_2 is most efficiently utilised over the Pt–Ce- and Ce-soot. The soot oxidation under the different feed gas conditions demonstrates that nitrate species are involved in the oxidation of Ce- and Pt–Ce-soot. The oxidation species with the decreasing order of activity are: (1) nitrates, (2) NO_2 , (3) lattice oxygen, and (4) gas-phase oxygen. All the above species are involved in the oxidation of Pt–Ce-soot.

KEY WORDS: diesel soot; fuel-borne catalyst; Pt; Ce; mechanism.

1. Introduction

Diesel engine exhaust gases contribute significantly to urban and global air pollution and despite emissions of hydrocarbon (HC) and CO from diesel exhaust gases are low and those can be easily converted by using a diesel oxidation catalyst (DOC) [1]. Though the improvements in the modern diesel engine design and combustion process will lead to decreased emissions of both NO_x ($NO + NO_2$, mainly present as NO) and particulates (soot or carbon particulates), these are not enough to meet the future legislations. During most of the diesel engine operation period the exhaust gas temperatures are around 300 °C and that temperature is too low for initiating continuous un-catalysed soot oxidation with O_2 or NO_2 [2]. Therefore, the heat necessary for soot burning is generated by diesel fuel oxidation (active regeneration), which is an inefficient process. From energy considerations and system design, an ideal particulate removal unit would minimise the temperature for continuous or induced regeneration of the soot filter. The two most popular technologies to decrease the soot oxidation temperature and, thereby, the energy requirement are: (i) catalysed soot filter that converts NO to NO_2 which in turn oxidises soot [3], and (ii) fuel-borne catalyst (FBC), that oxidises the soot mainly with O_2 as well as to some extent with NO [4]. The soot oxidation with oxygen is insignificant in a catalysed soot filter; this mainly arises due to from the poor contact between the catalyst and the soot [5].

The most widely implemented diesel particulate filters (DPF) for the passenger cars are developed by PSA, which meet the Euro IV particulate matter PM emission

standards [4]. This DPF system uses ceria or ceria-iron based fuel-borne catalysts and a silicon carbide (SiC) wall flow filter to collect and oxidise PM. Either injecting the fuel to increase the temperature of the filter can regenerate the filter or under certain driving conditions the FBC alone is able to perform filter regeneration. Using a fuel-borne catalyst the major problem of contact between catalyst and soot is overcome and un-catalysed soot filters can be used to capture and oxidise the soot. Depending on the type of fuel-borne catalysts used, the soot can be oxidised with O_2 or with $O_2 + NO_2$ [4,6,7]. The significant advantage of fuel-borne catalysts is further realised in the presence of SO_2 , which does hardly influence the soot oxidation behaviour. The FBC-DPF system is economic and reliable compared with catalysed soot filters. A variety of fuel-borne catalysts are proposed, the examples of fuel-borne catalysts studied are Ce, Fe, Ce–Fe, Pt, Pt–Ce, Mn, and Cu [4,6,7]. By utilising a combination of fuel-borne catalysts, the regeneration can be faster, ash built up can be small and also the balance-point temperature can be reduced. A balance-point temperature is the lowest temperature in a filter at which the amount of soot captured from the exhaust stream on the filter is in equilibrium with the amount of soot oxidised in the same time frame.

Though enough NO is present in the feed gas, the rate of NO oxidation to NO_2 over Ce or Ce–Fe fuel-borne catalysts is not efficient and, therefore, the more powerful oxidant (NO_2) cannot be extensively generated. Bimetallic fuel-borne catalysts containing ultra low concentrations of Pt–Ce has shown to decrease the balance point temperature to around 275–300 °C [6,7]. This is the lowest balance point achieved among the many combinations of fuel additives and catalysed soot

* To whom correspondence should be addressed.
E-mail: m.makkee@tudelft.nl

filters studied so far. The additional benefit by using a Pt–Ce fuel-borne catalyst is that it forms a Pt catalyst coating on the exhaust gas system and on the filter. This deposited Pt is able to significantly oxidise NO to NO₂ and, therefore, additionally decrease in the balance-point temperature is observed. Further advantages of using the Pt–Ce fuel-borne catalysts include the resistance to sulphur poisoning. Using the ultra low dosage of Pt–Ce (< 8 ppm) fuel-borne catalyst the frequency of a filter cleaning could be reduced significantly due to less ash accumulation. This will have significant advantage over a catalysed soot filter.

2. Experimental

2.1. Materials and characterisation

Ce (50 ppm), Pt (50 ppm), Pt–Ce-soot (2 ppm Pt and 30 ppm Ce), Cu-soot (100 ppm), and Fe (44 ppm) containing soot are generated from the respective fuel-borne catalyst additives (concentration given in parenthesis is the amount added to the fuel) in a real diesel engine [6,7]. The diesel engine used for the soot collection (at 75% load) and the filter evaluation was a two cylinder LPW2, produced by Lister-Petter, UK, and did not fulfil the Euro emission standards. The diesel fuels that were used during the programme were standard EN590 fuels (~500 ppm sulphur), summer specification, and Shell V-Power Diesel (< 10 ppm sulphur). The metal fuel additives used in the project are listed in Table 1. Soot samples are collected by maintaining the back pressure of the exhaust system at 0.5 bar using a slipstream valve. The collected soot was scraped of the filter and sieved with a 250 µm sieve.

Printex-U from Degussa S.A. is used as a model soot for the comparison of the oxidation rates. About 2.5 wt% Pt/Al₂O₃ (Pt/Al₂O₃) catalyst is obtained from Engelhard Corporation, USA. Ce(NO₃)₃·6H₂O is used as a catalyst to study soot oxidation in a tight contact with the catalyst (prepared by mixing the cerium nitrate and soot in a mortar) in DRIFT cell connected to mass spectrometer MS. Selected soot samples are characterised by XRD analysis.

2.2. Soot oxidation

Soot oxidation in 100 ml/min air is studied in a thermo-gravimetric analyser (TGA/SDTA851°, Mettler Toledo), from room temperature RT up to 800 °C with

a 10 °C/min heating rate. The soot sample was diluted with excess of silicon carbide in order to minimise the influences of heat and oxygen mass transfer phenomena on the soot oxidation rates.

A loose contact mixture of 80 mg of Pt/Al₂O₃ (when used) and 20 mg of soot (with and with out fuel-borne catalyst), mixed with a spatula and diluted with 400 mg of SiC is packed between two quartz wool plugs in a tubular quartz reactor. Soot oxidation is studied with 200 ml/min of 10 vol% O₂ or NO_x + 10 vol% O₂ in Ar. A (non-dispersed infra-red) NDIR analyser is used to monitor the reactant and product gases CO₂, CO, and NO. NO₂ is calculated from the difference of NO inlet and outlet concentrations.

3. Results

The X-ray diffractograms of the catalyst-soot samples as shown in figure 1a indicate that diffraction peaks correspond to the fuel-borne catalyst in addition to the diffraction bands of graphite sheets. The Pt-soot, generated from 50 ppm Pt additive, shows sharp diffraction peaks corresponding to Pt°. This indicates that there are large Pt particles present in the range off over 10 nm. In the Pt–Ce-soot, generated from 2 ppm Pt to 30 ppm Ce additive in from a fuel containing 500 ppm sulphur, prominent diffraction peaks, corresponding to Ce₂(SO₄)₃ and weak peaks corresponding to CeO₂, are evident. The diffractions, corresponding to Pt, are not observed in the Pt–Ce-soot. The Pt–Ce-soot is oxidised in 5000 ppm NO₂ + 10 vol% O₂ in Ar at 350 °C in order to see the changes that occur in the soot and the fuel-borne catalyst structure due to the progressive soot burning (figure 1b). Essentially all diffraction peaks, that are observed in the original Pt–Ce-soot, are present in the 70% oxidised Pt–Ce-soot with an increased intensity. The important observation is that even in 70% oxidised soot significant diffractions due to graphitic sheets are present.

All fuel-borne catalysts have shown a significant increase in the soot oxidation activity compared to an un-catalysed printex-U soot oxidation (figure 2). Generally, the Pt containing catalysts do not show an improved oxidation. In the present study Pt, however, is present as large crystallites in the over 10 nm range and such a large Pt crystallite is able to oxidise the soot. A relatively larger improvement in soot oxidation rates can be observed over the Fe-soot and Pt–Ce-soot compared to the Pt-soot and printex-U soot. Retaillieu *et al.* [8] have shown that around 50% of the fuel-borne catalyst ends up as sulphate, which on heating decomposes to Ce₂O₂S like phase that is capable for the soot oxidation. However, from XRD no such transformation was evident in the present study and the majority of fuel-borne catalyst ended up as cerium sulphate, even after 70% soot conversion in the presence of NO₂. Though the

Table 1
Fuel-borne catalysts and its source

Metal	Additive
Pt	Platinum Platinum Plus 3100
Ce	Cerium Rhône-Poulenc DPX9
Cu	Copper Lubrizol OS-96401
Fe	Iron Aldrich Ferrocene

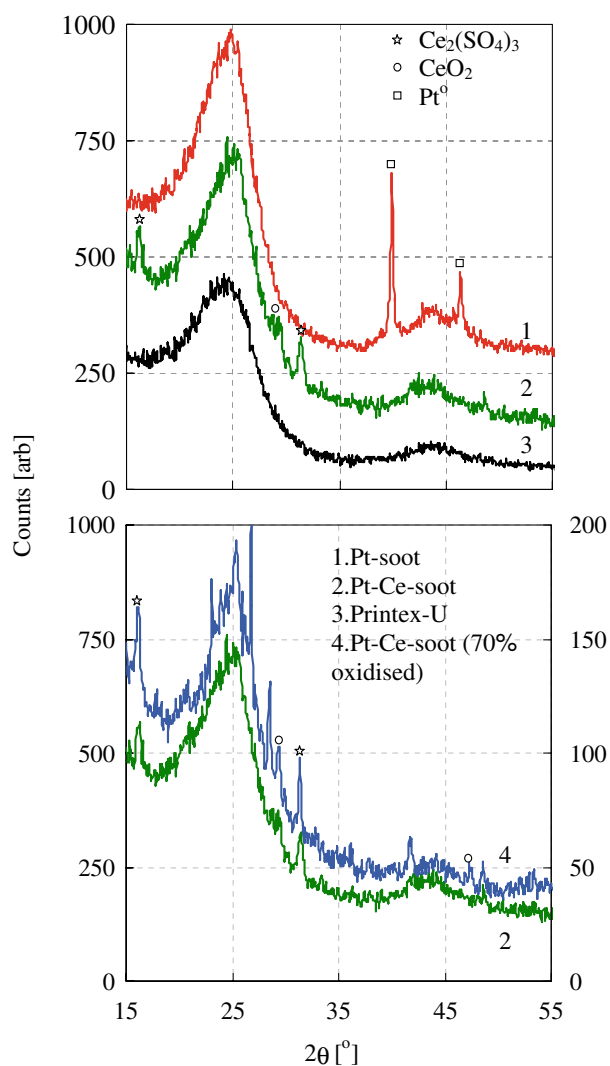


Figure 1. (a) XRD spectra of fresh soot samples as indicated; and (b) comparison of fresh Pt–Ce-soot and 70% oxidised Pt–Ce-soot. About 70% oxidised Pt–Ce-soot XRD spectra are collected under different instrument settings.

Fe-soot was not characterised by XRD, considering 500 ppm sulphur present in the fuel used for generating Fe-soot it can be expected that the Fe to some extent also forms sulphate. Furthermore, since Fe being a low atomic weight element, 44 ppm fuel additive will lead to significantly higher iron to carbon ratio in the final Fe-soot and part of the superior activity of the Fe-soot can be attributed to this higher molecular ratio. Compared to the Ce-soot alone, the presence of the Pt–Ce-soot improved the oxidation activity. The soot oxidation followed the trend in decreasing activity: Fe-soot > Pt–Ce-soot > Pt-soot ≥ Ce-soot > printex-U in the absence of NO_x in the gas phase.

Figure 3 shows fuel-borne catalyst-soot oxidation during the temperature ramping in the presence of 600 ppm $\text{NO} + 10 \text{ vol}\% \text{O}_2$ in Ar. Among the fuel-borne catalysts, the oxidation activity decreased in the order of Pt-soot > Pt–Ce-soot > Ce-soot > un-catalysed

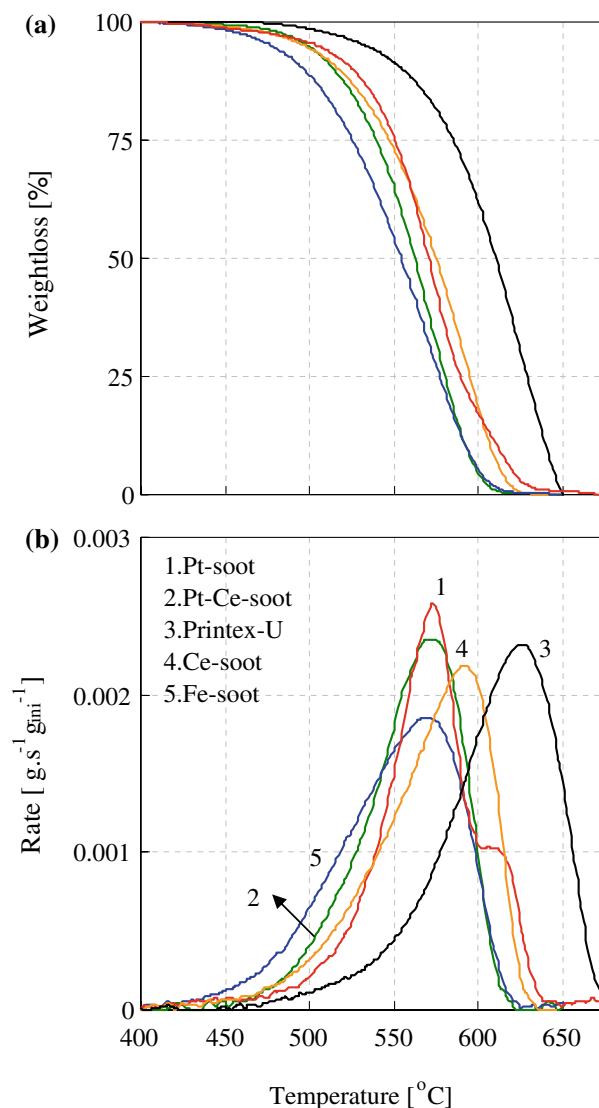


Figure 2. (a) Weight loss with temperature during soot oxidation with air; and (b) normalised soot oxidation rates. Reaction conditions: reactor-TGA, feed gas – 100 ml/min air, heating rate – 10 °C/min.

soot oxidation. It is interesting to note that the Pt-soot is the least active soot in the presence of O_2 alone, compared to Pt–Ce-soot, whereas it is significantly superior in the presence of NO . The main responsible oxidant for the decreasing in the soot oxidation temperature over the Pt-soot is the NO_2 generated over the Pt crystallites. Figure 4a shows the NO_2 slip during the soot oxidation as shown in figure 3. The Pt-soot generated significant amounts of NO_2 slip compared with the Pt–Ce-soot and Ce-soot. It can be expected that for the Pt–Ce-soot and Ce-soot due to the lower NO oxidation rates the generated NO_2 is completely utilised for the soot oxidation. The trend in the NO_2 slip followed the order Pt-soot > Pt–Ce-soot > Ce-soot > un-catalysed soot and from the NO_2 slip comparison it can also be stated that the Pt–Ce-soot and Ce-soot are less active than Pt-soot in the NO oxidation to NO_2 , but the generated NO_2 is more efficiently utilised in the soot oxidation over the former catalysts.

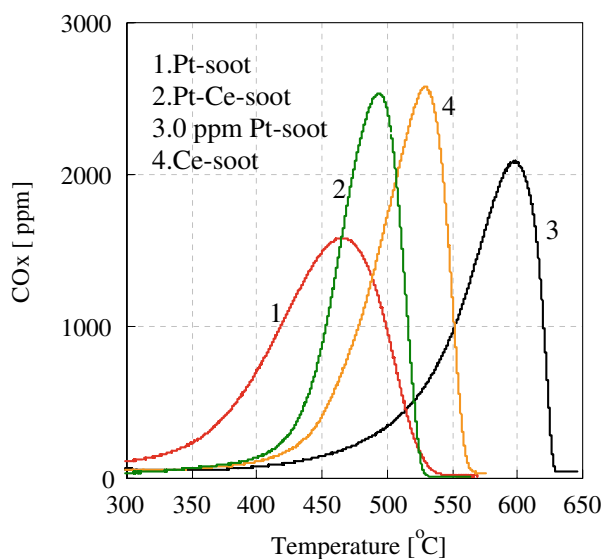


Figure 3. CO_x evolution with temperature during soot oxidation with $\text{NO} + \text{O}_2$, with increasing oxidation temperature. Reaction conditions: reactor-fixed bed, feed gas – 200 ml/min 600 ppm $\text{NO} + 10$ vol% $\text{O}_2 + \text{Ar}$, heating rate – $1^\circ\text{C}/\text{min}$, soot – 20 mg.

Before NO oxidation to NO_2 shown in figure 4b, the fuel-borne catalysts were exposed to 650°C during soot oxidation experiment to completely removal of the soot. Based on NO_2 slip (figure 4a) it was expected that Pt would be more active for NO conversion to NO_2 in the absence of soot (figure 4b) compared to the presence of soot (figure 4a). It was, however, less active. On the other hand, the activity of the NO oxidation over the Pt–Ce fuel-borne catalysts is clearly higher than that of NO_2 slip and Ce fuel-borne catalyst did not show a significant oxidation activity. The observed NO oxidation trends over fuel-borne catalysts suggest that Pt alone as fuel-borne catalyst seems to sinter extensively after complete soot oxidation compared with Pt–Ce and Ce alone are not very active for the NO oxidation to NO_2 . Based on the NO oxidation studies it is suggested

that the main function of the Ce component in the Pt–Ce-soot is to stabilise Pt crystallites. These crystallites will mainly convert NO to NO_2 resulting in an improved soot oxidation.

Figure 5 shows the oxidation of the fuel-borne catalyst-soot samples after the addition of 2.5 wt% $\text{Pt}/\text{Al}_2\text{O}_3$ in the presence of 600 ppm $\text{NO} + 10$ vol% O_2 in Ar . Because the $\text{Pt}/\text{Al}_2\text{O}_3$ is mixed with the fuel-borne catalyst-soot, a continuous supply of NO_2 can be ensured for soot oxidation and this will eliminate NO_2 dependence on fuel-borne catalyst. A completely different trend of the soot oxidation activity is observed compared to the oxidation in the presence of $\text{NO} + \text{O}_2$ or O_2 . Even the printex-U soot and Fe-soot are much more easily oxidised compared with the Pt-soot in the presence of $\text{Pt}/\text{Al}_2\text{O}_3$. No significant differences are found in the NO_2 slip between different combinations of fuel-borne catalyst-soot- $\text{Pt}/\text{Al}_2\text{O}_3$ mixtures, as the $\text{Pt}/\text{Al}_2\text{O}_3$ determines most of the soot oxidation activity (figure 5b). In the presence of the $\text{Pt}/\text{Al}_2\text{O}_3$ the soot oxidation trend is in the following order; Pt–Ce-soot > printex-U soot > Fe-soot > Pt-soot in the presence of NO_x in the gas phase.

Figure 6a shows the soot oxidation activity in the presence of 5000 ppm NO_2 at 350°C over the Pt–Ce-soot and printex-U soot. Both soot samples have shown a similar oxidation activity as evident from the similar CO_x concentration levels at the reactor outlet. Figure 6b shows the oxygen mass balance during the reaction over the Pt–Ce-soot. The oxygen mass balance between $\text{CO}_2 + \text{CO}$ at the reactor out let is similar to the NO concentration at the reactor outlet and, therefore, it can be concluded that the entire CO_x is arising from NO_2 . Figure 7 shows the temperature ramping experiments over the fuel-borne catalyst-soot samples with NO_2 , taken from the Ph.D. thesis of Jelles [9]. The Ce-soot and Cu-soot have shown a similar activity, whereas the Fe-soot shows a reduced activity. From the above isothermal and ramping experiments it can be argued that,

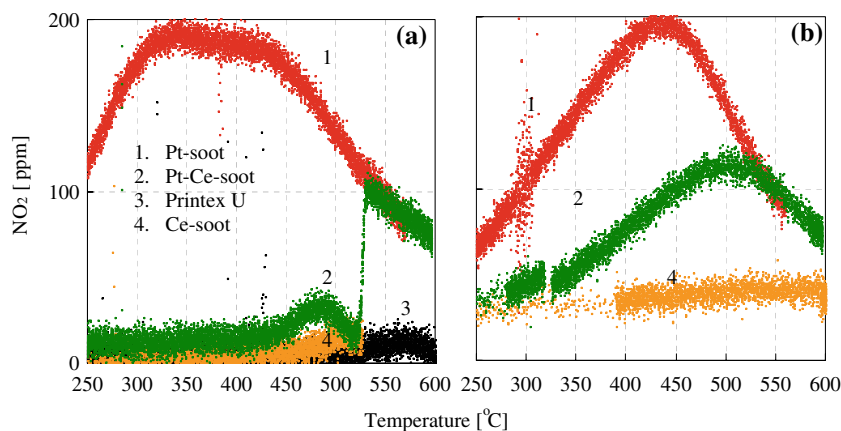


Figure 4. (a) NO_2 at the reactor outlet during soot oxidation (figure 3) and (b) NO_2 at the outlet after soot oxidation while cooling. Reaction conditions: reactor-fixed bed, feed gas – 200 ml/min 600 ppm $\text{NO} + 10$ vol% $\text{O}_2 + \text{Ar}$, heating rate – $1^\circ\text{C}/\text{min}$, soot – 20 mg. $\text{NO}_2 = \text{inlet} - \text{outlet}$ reactor NO concentrations measured by NDIR.

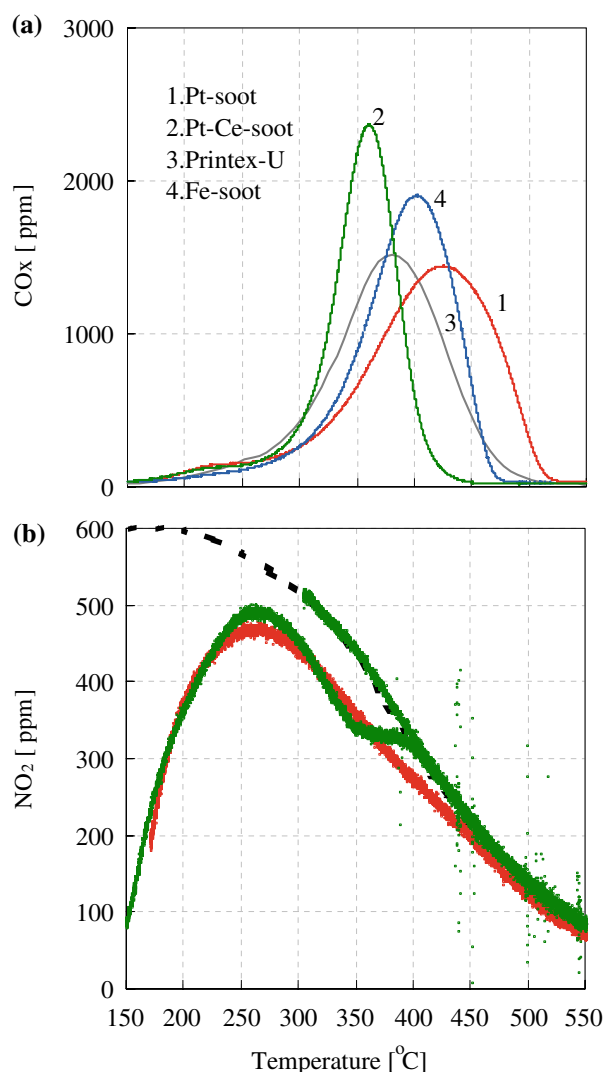


Figure 5. (a) CO_x; and (b) NO₂ at the reactor outlet with increasing temperature during soot oxidation with NO + O₂ + Pt/Al₂O₃. Reaction conditions: reactor-fixed bed, feed gas – 200 ml/min 600 ppm NO + 10 vol% O₂ + Ar, heating rate – 1 °C/min. Soot (20 mg) and Pt/Al₂O₃ (80 mg) are mixed with a spatula + silicon carbide as a diluent.

if the NO₂ is the only oxidant, fuel-borne catalysts do not play a significant role in the determination of the soot oxidation performance, in agreement with the proposal that the NO₂ reaction with the soot is un-catalysed.

Figure 8 shows the soot oxidation with 5000 ppm NO₂ + 10 vol% O₂ at 350 °C over the Pt–Ce-soot and printex-U soot. The CO_x concentration at the reactor outlet increased over both soot samples compared with the oxidation using NO₂ alone due to the Pt–Ce catalysed soot oxidation, to some extent using O₂, as an oxidant. The extent of the increase cannot, however, be explained based on either the NO recycle to NO₂ and the direct soot oxidation with O₂, catalysed by Ce.

Figure 9 shows the oxidation of soot mixed with Pt/Al₂O₃ at 350 °C in the presence of NO + O₂ in the feed

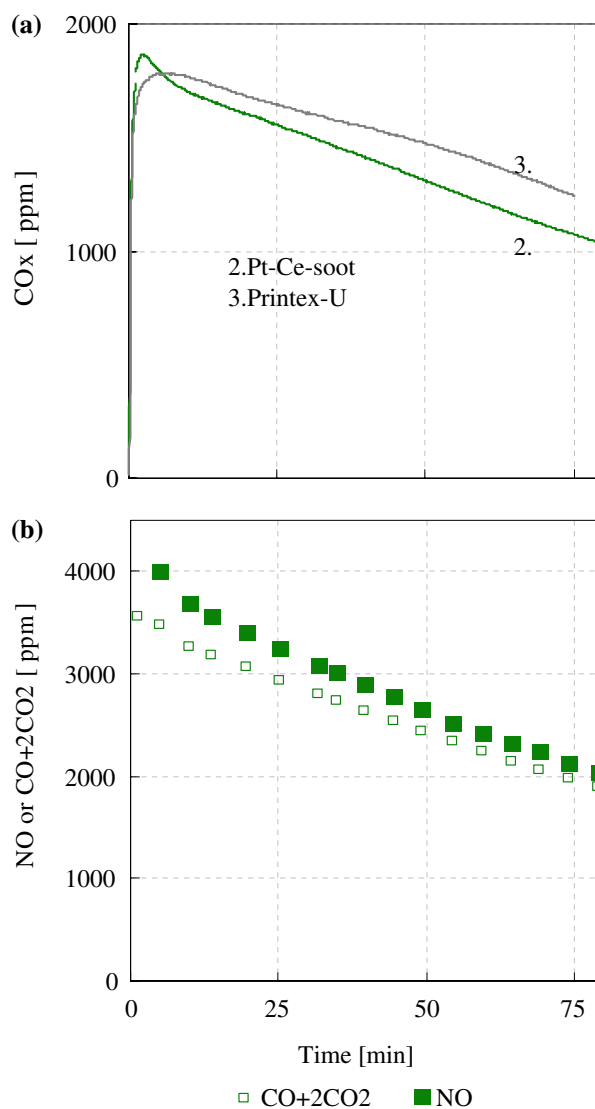


Figure 6. (a) CO_x over Pt–Ce-soot and Printex-U soot; and (b) oxygen mass balance (NO and 2CO₂ + CO) over Pt–Ce-soot during isothermal soot oxidation with NO₂ at 350 °C. Reaction conditions: reactor-fixed bed, feed gas – 200 ml/min 5000 ppm NO₂ + Ar, soot – 20 mg.

gas. The Pt–Ce-soot has shown a significantly higher soot oxidation activity compared with the rest of the soot samples despite of a similar or higher amount of fuel-borne catalyst present in the Pt-soot and Ce-soot samples. Various possibilities should be considered to explain the superior performance of Pt–Ce-soot and Ce-soot: (i) the main oxidant for the oxidation of the different soot samples is NO₂, (ii) NO₂ is mainly produced over the Pt/Al₂O₃ and the fuel-borne catalyst has very small influence if any and, so (iii) the NO recycle over the Pt–Ce-soot as a reason for the improved activity can be ruled out, as all the fuel-borne catalyst-soot compositions have this ability to produce NO₂ from the externally added Pt/Al₂O₃ catalyst. If this has to be an important step then the Pt-soot should show a significantly higher soot oxidation activity.

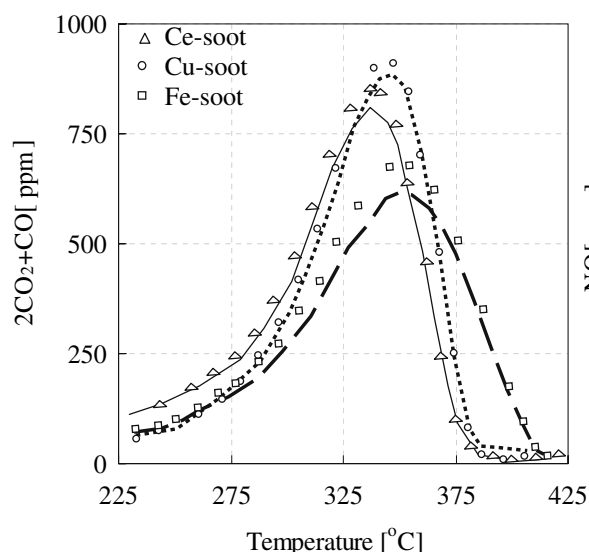


Figure 7. Catalyst-soot oxidation with NO_2 with increasing temperature. Reaction conditions: reactor-fixed bed, feed gas – 200 ml/min 2500 ppm NO_2 + Ar, heating rate – 0.2 °C/min, soot – 20 mg.

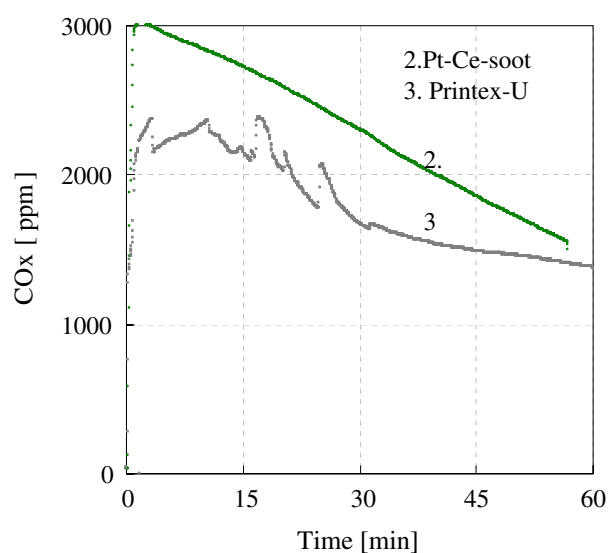


Figure 8. CO_x over Pt–Ce-soot and Printex-U soot during isothermal soot oxidation with NO_2 + O_2 at 350 °C. Reaction conditions: reactor-fixed bed, feed gas – 200 ml/min 5000 ppm NO_2 + 10 vol% O_2 + Ar, soot – 20 mg.

The superior oxidation performance of the Pt–Ce-soot and Ce-soot is only observed in the presence of excess NO_2 + O_2 or NO + O_2 + Pt/ Al_2O_3 . In order to explain such a behaviour especially in the presence of Pt/ Al_2O_3 catalyst Jelles *et al.* [6,7,9] have proposed that ceria catalyses the soot oxidation by NO_2 (apart from direct soot oxidation with NO_2). The NO_2 decomposes over CeO_2 to NO and adsorbed O^* on CeO_2 surface and the adsorbed O^* will efficiently oxidise the soot. If the above mechanism is operating, then Pt–Ce-soot could have shown a superior activity with NO_2 alone as

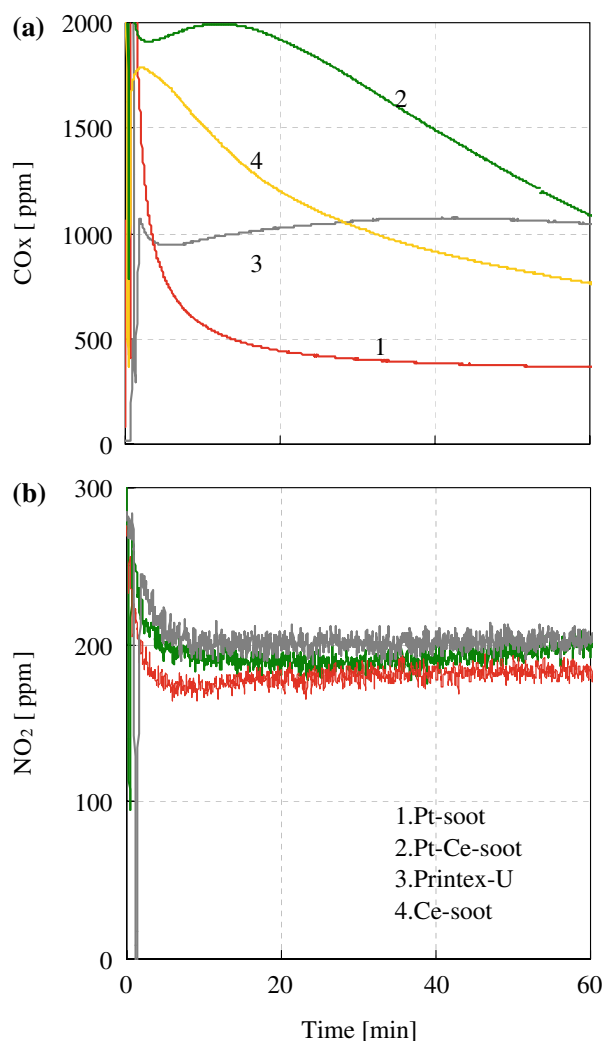


Figure 9. (a) CO_x , and (b) NO at the reactor during Pt–Ce-soot and Printex-U soot oxidation with 300 ppm NO + O_2 at 350 °C. Reaction conditions: reactor-fixed bed, feed gas – 200 ml/min 300 ppm NO_2 + 10 vol% O_2 + Ar, soot – 20 mg.

an oxidant compared with the other fuel-borne catalyst-soot samples. This is, however, not the case. Therefore, there should be another mechanistic routes of the soot oxidation to explain the superior performance of Pt–Ce-soot in the presence of NO_2 + O_2 or NO + O_2 + Pt/ Al_2O_3 . Under these feed gas conditions one can expect apart from the known gas-phase species the formation of surface nitrates on ceria. Decomposition products of nitrates are very powerful oxidants in the soot oxidation. Because the ceria is in a tight contact with the soot the transfer of decomposed nitrates to soot surface should be efficient.

Figure 10 shows the decomposition of $\text{Ce}(\text{NO}_3)_3$ and $\text{Ce}(\text{NO}_3)_3$ + soot (4:1 tight contact mixture due the mixing in a mortar) in He in a DRIFT cell connected to mass spectrometer MS. The cerium nitrate precursor decomposition alone gives NO_2 + O_2 in the gas phase ($2\text{Ce}(\text{NO}_3)_3 \rightarrow 2\text{CeO}_2 + 6\text{NO}_2 + \text{O}_2$) (figure 10a). In the presence of the soot, cerium nitrate decomposed at a

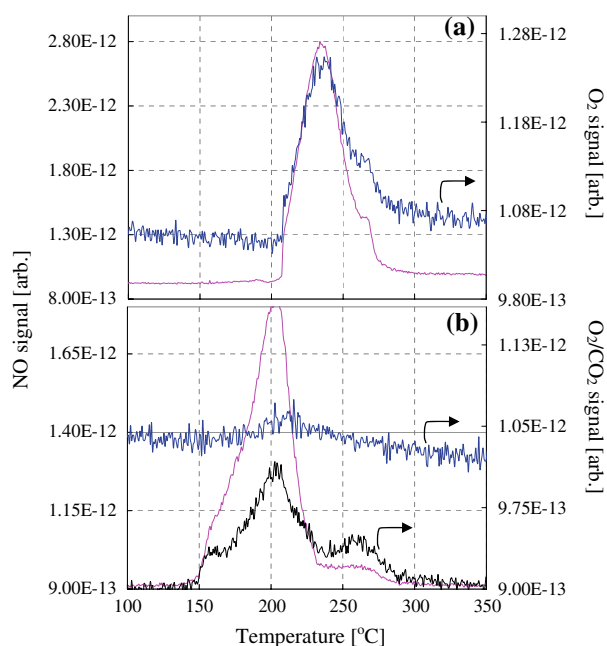


Figure 10. MS analysis of (a) $\text{Ce}(\text{NO}_3)_3$, and (b) $\text{Ce}(\text{NO}_3)_3 + \text{Printex-U}$ soot decomposition in He. Reaction conditions: reactor-DRIFT cell connected to MS, feed gas – 20 ml/min He, $\text{Ce}(\text{NO}_3)_3 + \text{soot}$ were ground in a mortar.

lower temperature due to its reaction with the soot and no oxygen is observed (figure 10b). The absence of oxygen clearly indicates that nitrate is a primary reactant at these low temperatures around 200 °C.

4. Discussion

The mechanistic aspects of the soot oxidation over Pt/support type after-treatment systems are straightforward and are extensively reported in literature. The main oxidation function arises from the Pt crystallites, on which the exhaust gas NO is oxidised to NO_2 . This formed NO_2 will further react with the soot around 300 °C. As the NO conversion to NO_2 is both thermodynamically and kinetically controlled, the excess NO in the exhaust gas is necessary compared with soot ($\text{NO}/\text{soot} > 20$) in order to realise a significant soot oxidation around 300 °C [2]. The main disadvantages of the catalysed soot traps arise from their durability and resistance to the SO_3 poisoning, especially when used in heavy-duty applications. The fuel-borne catalysts in this respect have the advantages as the durability of the catalyst is not an issue, and SO_2 is found to have a very small influence compared with catalysed soot traps [6–9]. Though the fuel-borne catalysts have been studied for the past two decades, not many mechanistic aspects on how the soot is oxidised over these catalysts are not thoroughly studied. It is assumed that the oxygen storage capacity of ceria is capable of providing locally the necessary active species for the soot oxidation. However, the reaction/characterisation studies known limited to

correlate different catalyst surface properties with the soot oxidation activity, especially in the presence of $\text{NO} + \text{O}_2$. In the present study the fuel-borne catalyst-soot samples (Table 1), except the Pt-soot, are generated with a fuel containing 500 ppm of sulphur, and have been characterised. The reasons for the possible superior activity of Pt–Ce-soot compared with the other catalyst-soot samples are explained by different active species in the gas phase or on the fuel-borne catalyst.

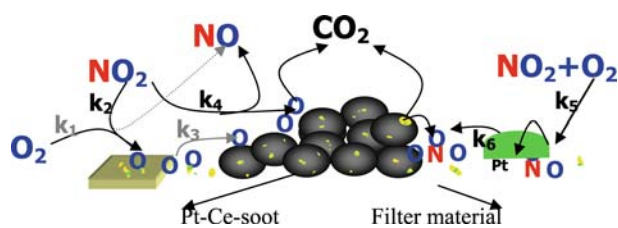
X-ray diffractograms of all soot samples essentially showed similar features (figure 1): large Pt crystallites are observed in the Pt-soot and $\text{Ce}_2(\text{SO}_4)_3$ and CeO_2 phases are observed in the Pt–Ce-soot. No XRD observable Pt crystallites are detected in the Pt–Ce-soot due to the ultra low dosage of Pt additive (2 ppm). No major changes of the cerium sulphate phases are observed even in 70% oxidised Pt–Ce-soot. Retailleau *et al.* [8] have observed the decomposition of cerium sulphate as an important step, forming new phases that can activate oxygen in the soot oxidation. However, such a significant transformation of the cerium sulphate is not evident from XRD in the present study and the $\text{Ce}_2(\text{SO}_4)_3$ phases can be considered as inactive phase in the soot oxidation experiments. It is shown that the surface lattice oxygen of CeO_2 is involved in the soot oxidation [10]. CeO_2 supplies the lattice oxygen efficiently to soot thus creating oxygen vacancies, which are quickly filled by gas-phase oxygen and further driving the soot oxidation. It is also important to notice that, even in the 70% oxidised Pt–Ce-soot, relatively significant diffractions due to graphitic sheets are observed (figure 1b). This indicates that the soot burning is first taking place on amorphous mass in the soot particle, followed by the consumption of the graphitic sheets. This suggests that the oxidation model may not follow shrinking core formalism. This observation indicates that during soot oxidation of fuel-borne catalyst-soot, if any of the catalyst particles are buried inside the primary particle, with progressive soot oxidation these particles are exposed and could potentially increase the oxidation rate.

Since the majority of the fuel-borne catalysts are present as cerium sulphate, it can be stated that Pt is significantly less active compared with the ceria-soot samples with O_2 (figure 2). On the other hand, in the presence of $\text{NO} + \text{O}_2$, the Pt-catalysts are significantly more active (figure 3a). The improved soot oxidation activity is obviously due to superior NO oxidation to NO_2 over the Pt-soot (figure 4a), which further oxidises soot to CO_2 . The Ce-soot is least active and the Pt–Ce-soot (considering low dosage of fuel-borne additive, 2 ppm Pt–30 ppm Ce) has shown moderate activity. From the higher NO oxidation to NO_2 in the presence of soot, compared with lower NO oxidation activity to NO_2 in the absence of soot over Pt, it can be concluded that Pt sinters in the absence of support after soot oxidation. On the other hand, the function of Ce in

Pt–Ce-soot seems to stabilise Pt crystallites towards sintering. Pt–Ce combination will have a significantly higher impact in increasing the soot oxidation rate compared to Pt alone which can be expected to extensively sinter.

When fuel-borne catalyst-soot is mixed with Pt/Al₂O₃ and the soot oxidation is carried out with NO + O₂, the Pt–Ce-soot is more reactive compared with all other soot samples (figure 5). The observed differences in the soot oxidation activity under these conditions cannot be explained based on the different extents of NO oxidation to NO₂. If the NO oxidation to NO₂ is the main reactant for the soot oxidation then the Pt-soot + Pt/Al₂O₃ is expected to show a higher soot oxidation activity. The enhanced soot oxidation over Pt–Ce-soot should, therefore, be either due to the different nature of the soot or due to the fuel-borne Pt–Ce catalyst. It was suggested that the NO₂ formed on the supported platinum catalyst will decompose to give NO and adsorbed 'O' on the Pt–Ce catalyst, and such an oxygen is responsible for the high soot oxidation activity [6]. However, all the soot samples have shown a similar activity in the presence of NO₂ alone (figures 6 and 7). If Pt–Ce is catalysing the soot oxidation with NO₂, then the Pt–Ce-soot is expected to show a significantly higher soot oxidation activity with NO₂. The significant superior activity over Pt–Ce-soot is only observed with NO₂ in the presence of O₂ (figure 8) or NO + O₂ + Pt/Al₂O₃ (figure 9). Even the Ce-soot is more reactive compared with the Pt-soot in the presence of NO + O₂ + Pt/Al₂O₃ (figure 9). This high activity can be hypothesised that the main reaction, that takes place under these reaction conditions, is the formation of the surface nitrates over the ceria. These nitrates are found to oxidise the soot at very low temperatures (around 200 °C) in comparison with the gas-phase NO₂ at around 300 °C (figure 10). Though CeO₂ alone is capable of forming the surface nitrates, the combination of Pt and Ce shows a synergetic effect and seems to improve the rate of such nitrate formation. On the other hand, the Fe-, Cu-, and Pt-fuel-borne catalysts do not form extensively these surface nitrates and the main reactions over these catalysts are the direct soot oxidation with NO₂ and O₂.

Based on the experimental results, the different reactions that are important for the soot oxidation are summarised in Scheme 1. It can be concluded that the oxidation activity of the species with the decreasing order is: (1) nitrates, NO₃⁻, (2) NO₂, (3) lattice oxygen, and (4) gas-phase oxygen. From the present study and that of Jelles *et al.* [6,7,9] the hypothesis is formulated that all possible oxidation species present in the exhaust gas and on the catalyst surface (Scheme 1) can be effectively utilised in Pt–Ce-soot oxidation in comparison with any of the known catalytic systems. Furthermore, the Pt in the ultimately formed Pt–Ce residue seems to be stable and with the ageing of the trap is



Scheme 1. Soot oxidation mechanism over Pt–Ce-soot generated from fuel-borne catalyst.

expected to improve the NO conversion to NO₂ significantly. There is still room for improvement in the fuel-borne catalyst activity, for example by decreasing the sulphur content present in the diesel fuel and, therefore, the inactive cerium-sulphate phases can be decreased and most of the ceria could be utilised for the soot oxidation through the nitrate route.

5. Conclusions

Fe-, Pt–Ce- and Ce-soot are oxidised at a lower temperature with O₂ compared with Pt-soot and the opposite trend is observed with NO + O₂. NO is oxidised to NO₂ more efficiently over the Pt-soot, whereas it is more efficiently utilised over the Ce- and Pt–Ce-soot samples. Soot oxidation under different feed gas conditions suggests that in the presence of NO₂ + O₂ nitrate species are involved in the oxidation over Ce- and Pt–Ce-soot samples. Different oxidation species with decreasing order of activity which are responsible for the fuel-borne catalysts, in general, are suggested as: (1) nitrates, (2) NO₂, (3) lattice oxygen, and (4) gas-phase oxygen. All the above species are involved in the oxidation of the Pt–Ce-soot which is the most easily to be oxidised soot under practical conditions.

References

- [1] R.J. Farrauto and K.E. Voss, *Appl. Catal. B: Environ.* 10 (1996) 29.
- [2] K. Kimura, T.L. Alleman, S. Chatterjee and K. Hallstrom, SAE paper 2004-01-0079 (Detroit, 2004).
- [3] R. Allnsson, C. Goersmann, M. Lavenius, P. Phillips, A.J. Uusimaki and A.P. Walker, SAE paper 2004-01-0072 (Detroit 2004).
- [4] T. Campenon, P. Wouters, G. Blanchard, P. Macaudiere and T. Seguelong, SAE paper 2004-01-0071 (Detroit, 2004).
- [5] J.P.A. Neeft, M. Makkee and J.A. Moulijn, *Chem. Eng. J.* 64 (1996) 295.
- [6] S.J. Jelles, R.R. Krul, M. Makkee, J.A. Moulijn, G.J.K. Acres and J.D. Peter-Hoblyn, SAE 1999-01-0113 (Detroit, 1999).
- [7] S.J. Jelles, M. Makkee and J.A. Moulijn, *Top. Catal.* 16 (2001) 269.
- [8] L. Retailleau, R. Vonarb, V. Perrichon, E. Jean and D. Bianchi, *Energy Fuels* 18 (2004) 872.
- [9] S.J. Jelles, Ph.D. Thesis (TU Delft, The Netherlands, 1999).
- [10] A. Bueno-Lopez, K. Krishna, M. Makkee and J.A. Moulijn, *J. Catal.* 230 (2005) 237.